ngVLA Antenna Memo # 10

Beam Pointing and Efficiency as a Function of Translations and Rotations of Optical Elements on the ngVLA Antenna

Sivasankaran Srikanth, Central Development Laboratory, Charlottesville, VA

September 4, 2020.

Abstract

This memo presents the direction of the beam and the resulting drop in efficiency of the ngVLA antenna as the feed, the subreflector and the main reflector move or rotate from their intended positions in/about 3 different axes. Pointing coefficients are computed for translations (arcmin/cm) and rotations (arcmin/arcmin).

1 Introduction

Figure 1 shows the optics layout of the ngVLA dual-offset shaped antenna (Version 6). The feed and/or the subreflector are/is likely to move/rotate from their original positions due to gravity, wind or thermal loading during operation. The amount of translation/rotation can be predicted in finite element modeling of the antenna. A knowledge of the change in pointing and loss in efficiency as a result of the translation/rotation is critical to ascertain if the antenna meets the specifications provided to the contractors. It also provides NRAO the metric for comparing antennas designed by different contractors.

Analysis was carried out between 12.3 and 20.5 GHz (Band 3) frequency range using GRASP software from TICRA. The analysis can be grouped into three categories: translation/rotation of (1) the feed, (2) the subreflector and (3) the feed and the subreflector as a unit. The last analysis is equivalent to the translations/rotations of the main reflector. Each of the element translation/rotation is done in its respective coordinate system shown in Figure 1. In the case of the subreflector, analysis of translation in the feed coordinate system has also been carried out. The limits of the translations/rotations used are where the resulting efficiency has dropped below 50%. However, in some cases the efficiency loss is very small even for sufficiently large rotations. All of the results shown are at 16.5 GHz.

2 Feed offsets/rotations

Figure 2 shows the pointing offset and ratio of off-axis to on-axis efficiency for translations up to 7.5 cm in three different axes at 16.5 GHz. The plane in which the telescope beam shifts is indicated in the graphs by the value of ϕ. Both the pointing offset and efficiency ratio are nearly the same for both X- and Y-axes translations, with efficiency dropping to 50% and the pointing offset to 20 arcmin (′) at a 7.5 cm offset. The graph is asymmetric by a small amount in the X-axis case (Figure 2 (a)). For translations in the Z-axis, there is no pointing offset; however, efficiency ratio drops to 10% for an offset of 7.5 cm. For feed rotations of ±6°, the efficiency drop is minuscule at 1.3%, 2% and 1.1% in X-, Y- and Z-directions, respectively, as shown in Figure 3. There is no pointing offset for these feed rotations.

3 Subreflector offsets/rotations

Figure 4 shows the results for subreflector translations in the feed coordinate system. The asymmetry in efficiency is large for the X-axis case, with the ratio at 58% at +5 cm and 46% at -5 cm. A translation of 5 cm in Y-axis results in efficiency ratio dropping to 43%. For 5 cm translation in both X- and Y-directions, pointing change is -25 arcmin. In the Z-direction, efficiency ratio drops to 12% and 19% even

for small translations of ±2.5 cm, with a pointing offset of about 4 arcmin at -2.5 cm. Figure 5 shows the pointing offsets and efficiency ratio for translations in the subreflector coordinate system. The efficiency ratio is 55% and 42% for the +5 and -5 cm translations in X, respectively, while in the Y-direction, the efficiency ratio is 43%. The pointing change is again ±25 arcmin in both X- and Y-directions. The efficiency is about the same for an offset in the Z-direction, as that in the case of offset in the feed coordinate system. The maximum pointing offset is about 3 arcmin.

Figure 6 shows the effect of subreflector rotations, which is much more adverse compared to that for feed rotations. For instance, for a rotation of 2° about the Y-axis, the efficiency drops by 69% and the pointing offset is about 19 arcmin. Rotation about the X-axis is more forgiving, with efficiency dropping by 52% and with a pointing offset of -9.6 arcmin. Rotation of 2° about the Z-axis results in efficiency loss of 12%, with a small pointing offset of <1 arcmin.

4 Main reflector offsets/rotations

Analysis with respect to the main reflector is carried out treating the feed and the subreflector as one integrated unit. Figure 7 shows the results of main reflector translations with respect to the feed arm that supports the feed and subreflector. In the Y-axis, for a 5 cm offset the drop in efficiency is 50%, better than the subreflector offset response by 7%. The pointing offset is 13 arcmin, half that of the subreflector case. However, for an offset of 5 cm in the X-axis, the efficiency drop is much higher at 71% compared to 45% for the subreflector. The drop in efficiency is about 62% for an offset of 5 cm along the Z-axis with the introduction of a pointing offset of 10.8 arcmin.

The drop in efficiency is greater than 80% for small rotations of ±0.5° about the X- and Y-axes, as shown in Figures 8(a) and 8(b). The pointing offset is higher for Y-axis rotations with a value of 55 arcmin for a +0.5° rotation. In the Z- direction, efficiency ratio drops below 30% for rotations >0.6° (Figure 8(c)).

5 Pointing coefficients

Pointing coefficients for translations (arcmin/cm) and rotations (arcmin/arcmin) are given in Table 1. In most cases, the pointing offset is a linear function of the position or orientation of the elements of the optics and in cases where it is not, pointing coefficient is calculated in the linear portion of the trace. Subreflector translations in the transverse directions result in the highest pointing coefficients, two times as that for feed translations. When the feed and subreflector move in the transverse plane as a unit, with respect to the main reflector, pointing offsets are again only half as that due to translation of the subreflector by itself. Main reflector rotation about the Y-axis results in a high value for the pointing coefficient.

6 Conclusion

Translations and rotations of the subreflector are more critical compared to those of the feed. The fact that the subreflector remains fixed on the feed arm is a silver lining. Translation due to gravity loading on the feed and subreflector as a unit is of less concern compared to rotations caused by gravity loading. However, translations caused by cross-wind loading on the subreflector may be something that needs careful attention.

The author acknowledges R. Selina and P. Ward for their valuable and constructive suggestions and edits.

Table 1. Pointing coefficients for translations (arcmin/cm) and rotations (arcmin/arcmin) of each optical element.

	Axis	Translation		Rotation
		arcmin/cm	BW/λ	arcmin/arcmin
Feed	X_f	2.6815	1.2549	0.0000
	Y_f	2.6850	1.2565	0.0000
	Z_f	0.000	0.0000	0.0000
Subreflector	X_s	-5.1850	-2.4264	-0.0879
	Y_s	-5.3604	-2.5085	0.1753
	Z_s	-0.6445	-0.3016	0.0068
Subreflector	X_f	-5.0030	-2.3412	
	Y_f	-5.3604	-2.5084	
	Z_f	-1.2900	-0.6037	
Main reflector	X	1.5697	0.7346	-0.7886
	Y	2.6864	1.2571	1.8153
	Z	2.1496	1.005 9	0.0495

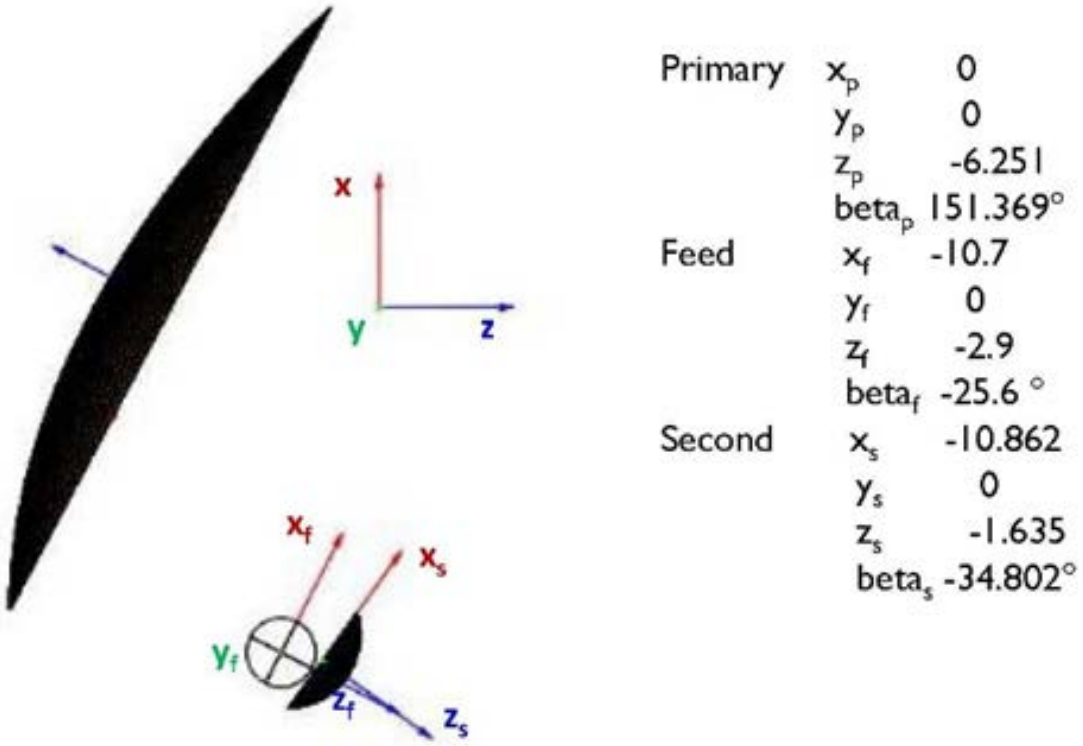

Figure 1. GRASP model of the ngVLA antenna

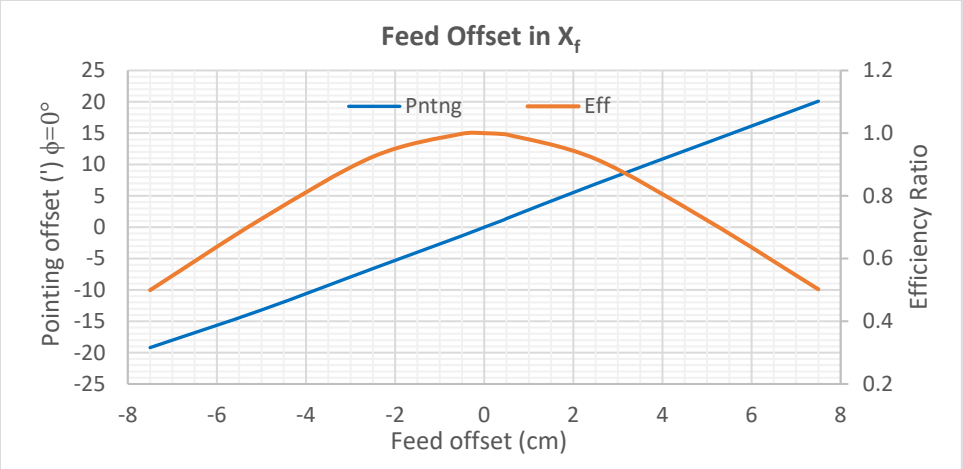

(a) Translation in X_f (±7.5 cm)

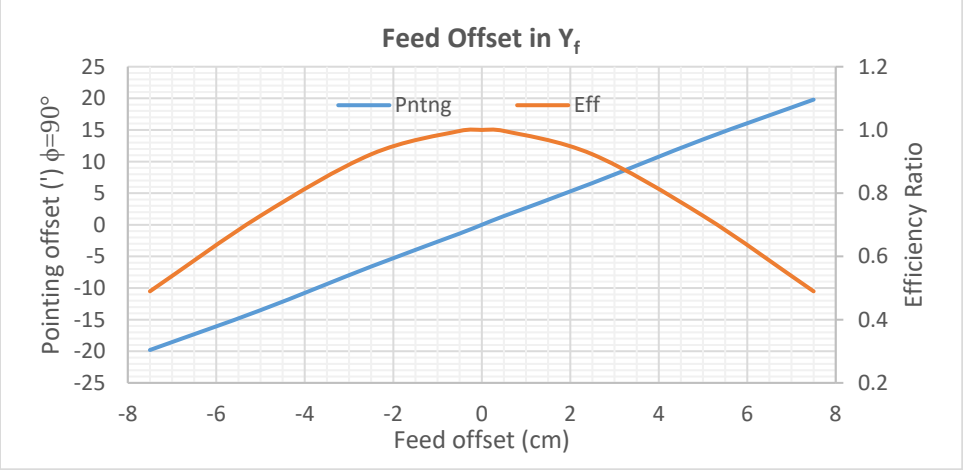

(b) Translation in Y_f (±7.5 cm)

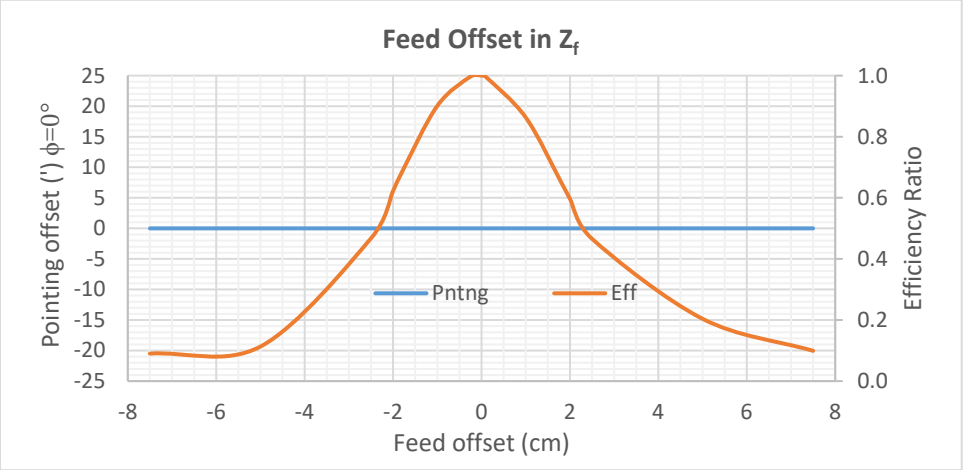

(c) Translation in Z_f (±7.5 cm)

Figure 2. Feed offsets.

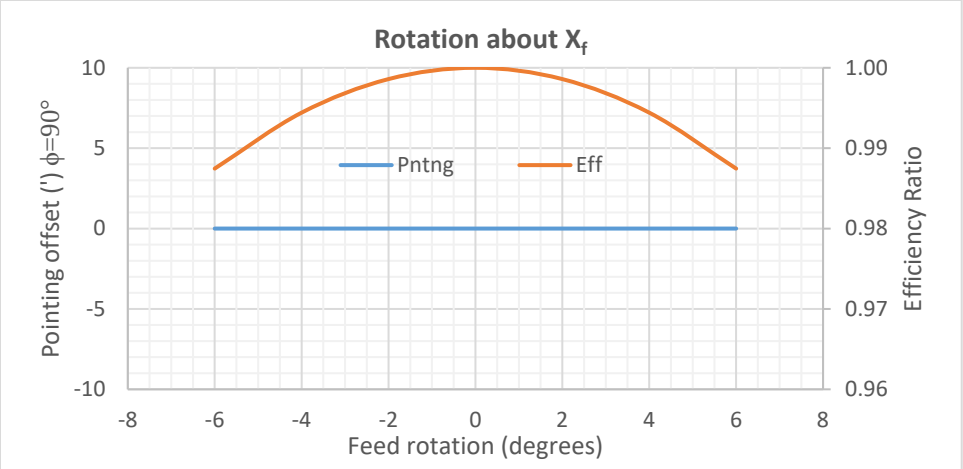

(a) Rotation about X_f (±6°)

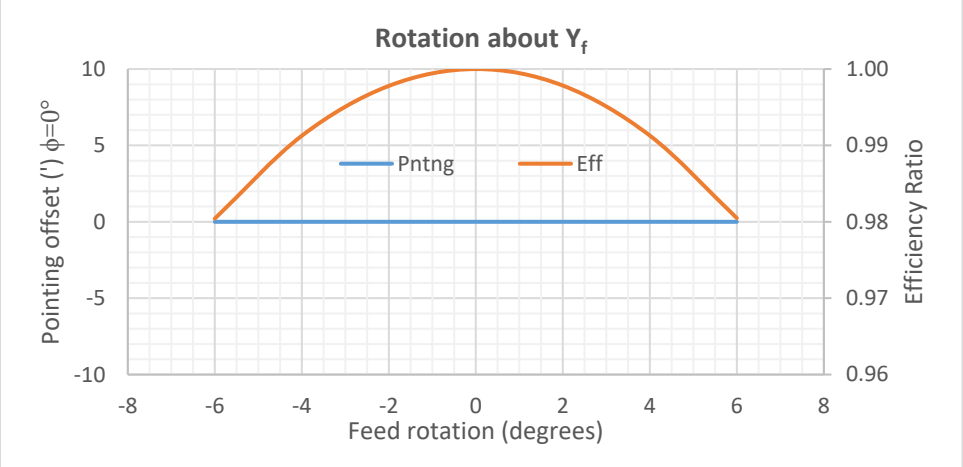

(b) Rotation about Y_f (±6°)

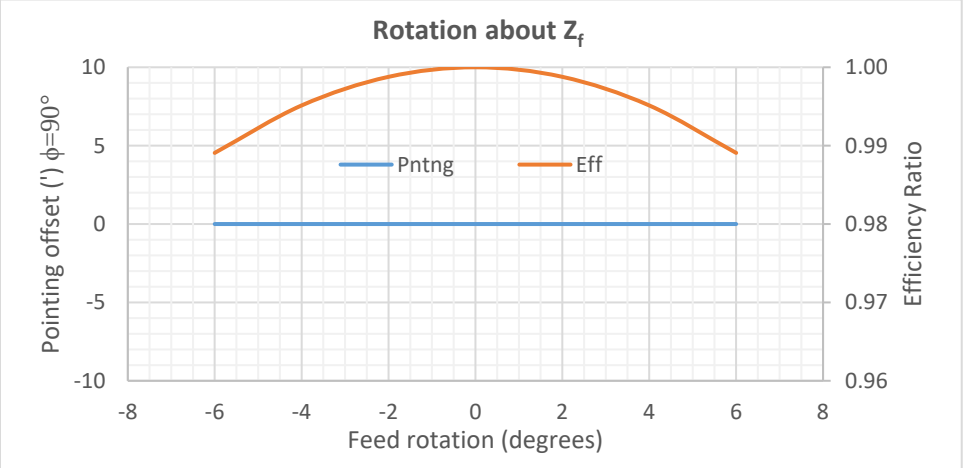

(c) Rotation about Z_f (±6°)

Figure 3. Feed rotations.

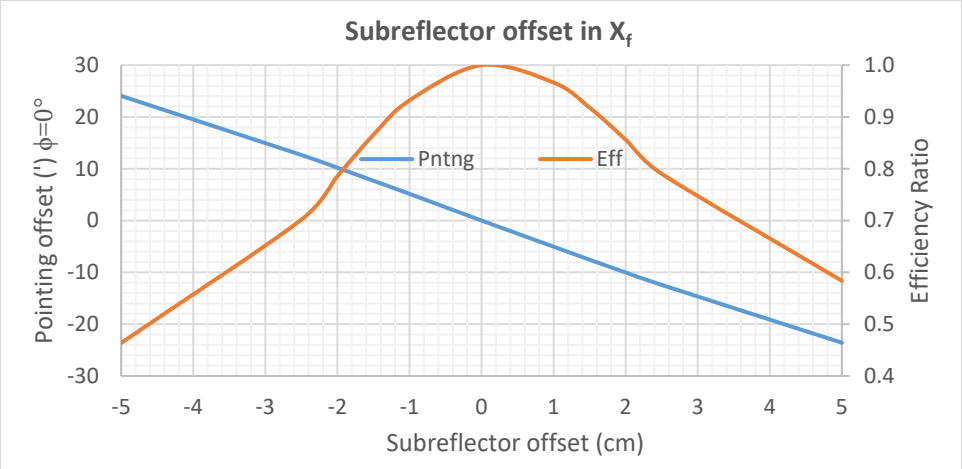

(a) Translation in X_f (±5 cm)

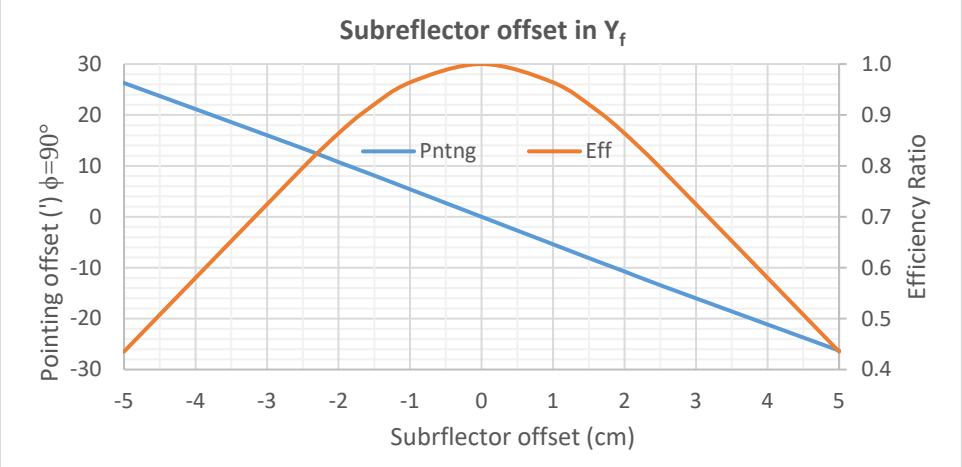

(b) Translation in Y_f (±5 cm)

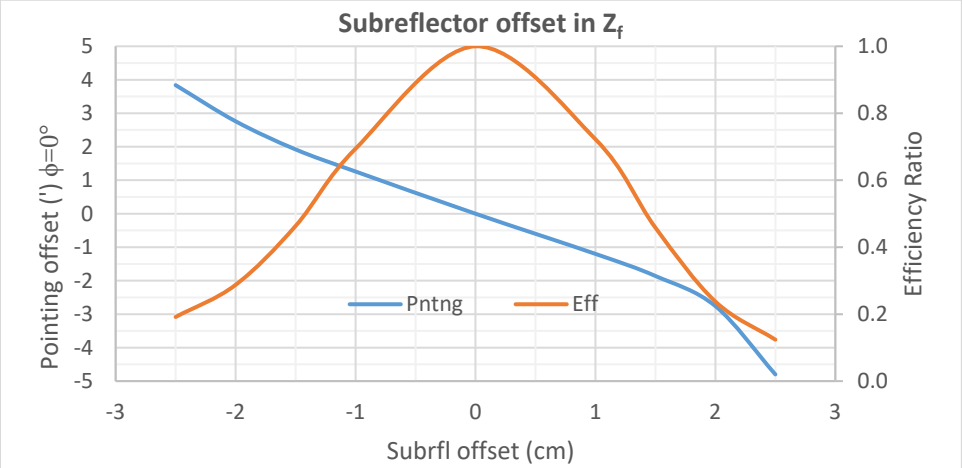

(c) Translation in Z_f (±3 cm)

Figure 4. Subreflector offsets in feed coordinates.

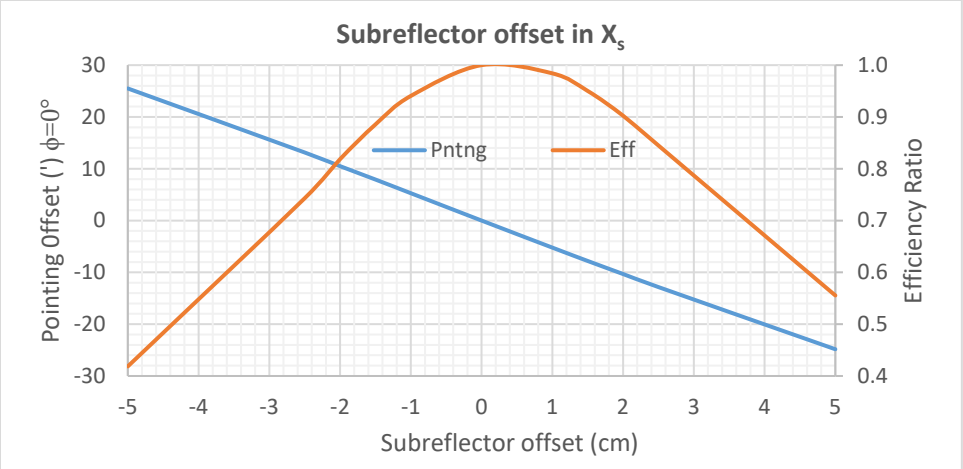

(a) Translation in X_s (±5 cm)

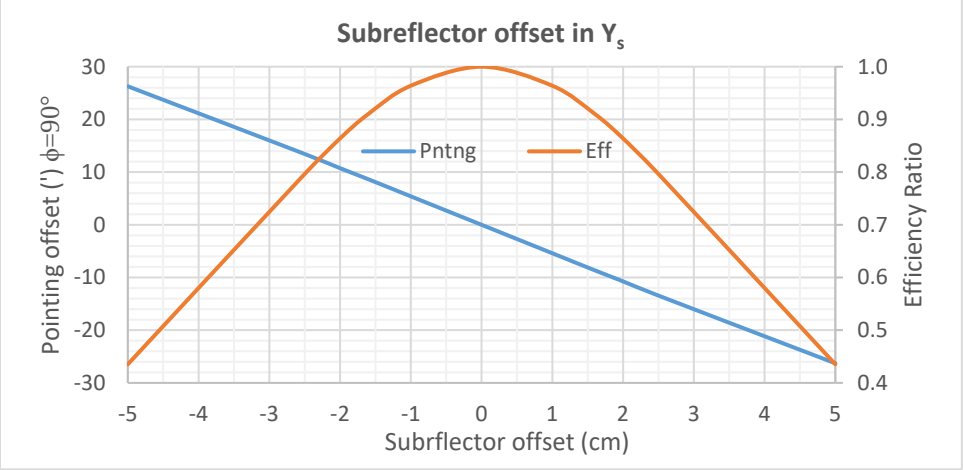

(b) Translation in Y_s (±5 cm)

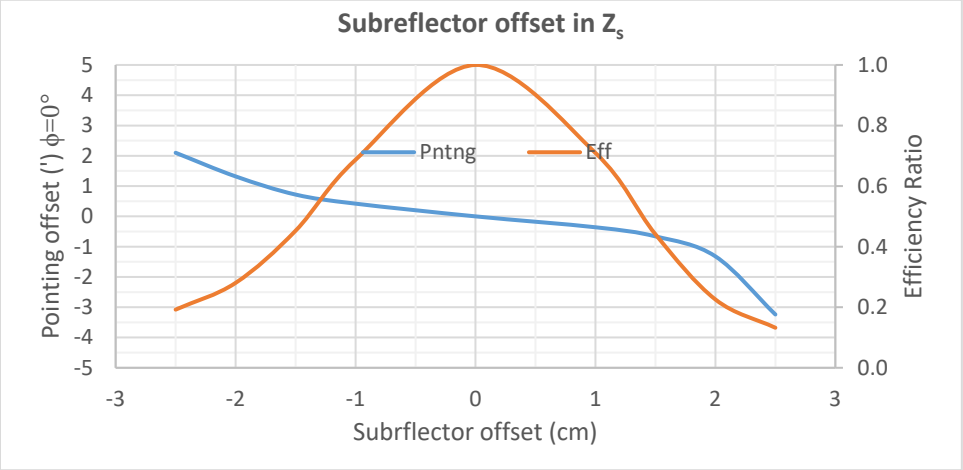

(c) Translation in Z_s (±3 cm)

Figure 5. Subreflector offsets in subreflector coordinates.

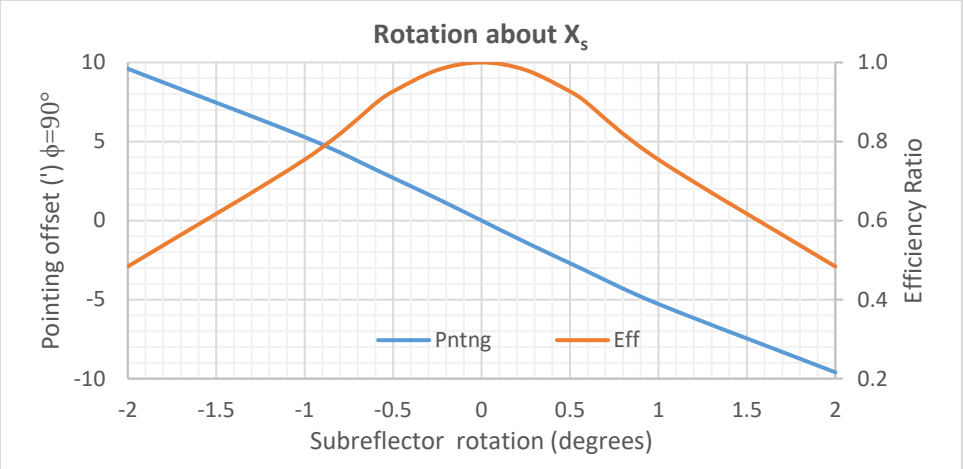

(a) Rotation about X_s (±2°)

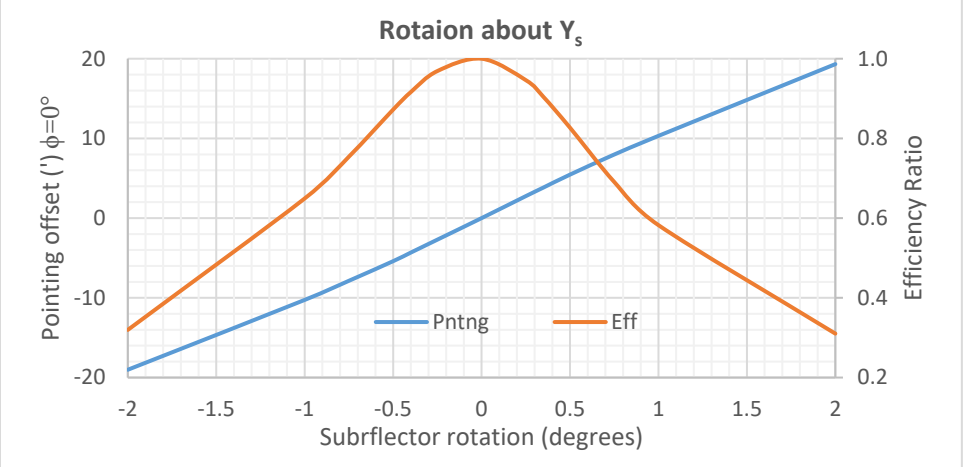

(b) Rotation about Y_s (±2°)

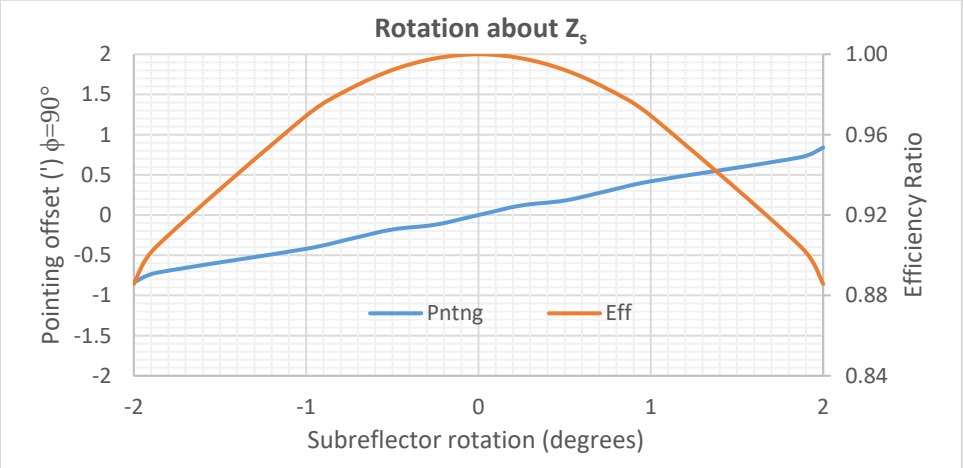

(c) Rotation about Z_s (±2°)

Figure 6. Subreflector rotations in subreflector coordinates.

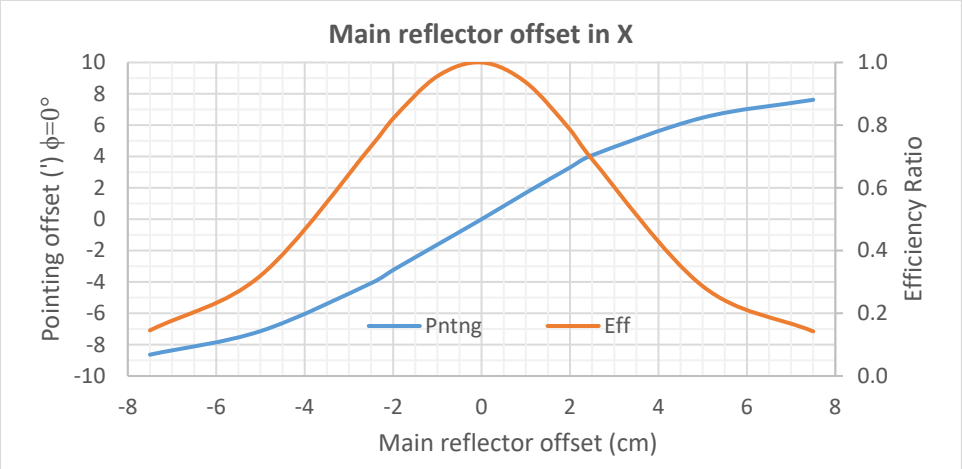

(a) Translation in X (±7.5 cm)

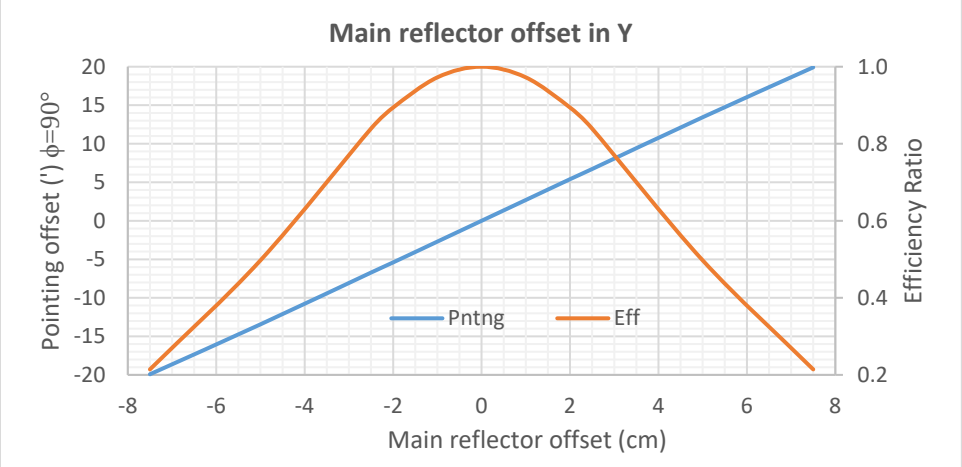

(b) Translation in Y (±7.5 cm)

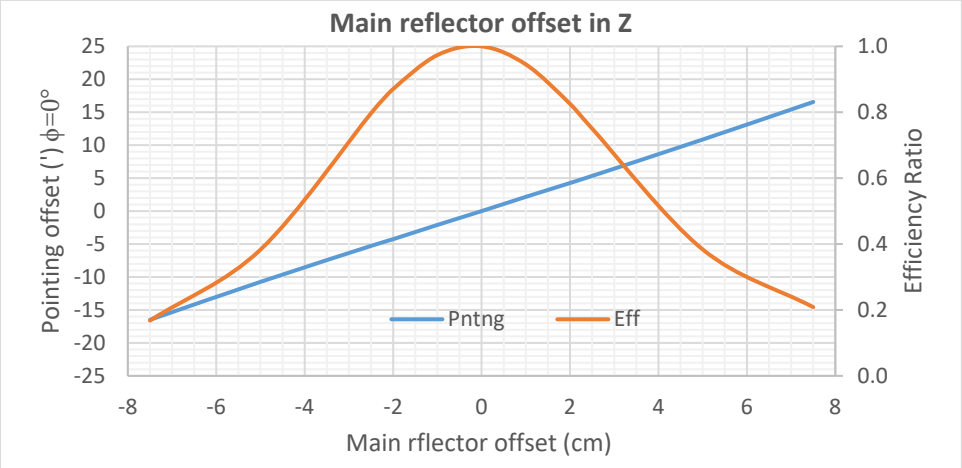

(c) Translation in Z (±7.5 cm)

Figure 7. Main reflector offsets.

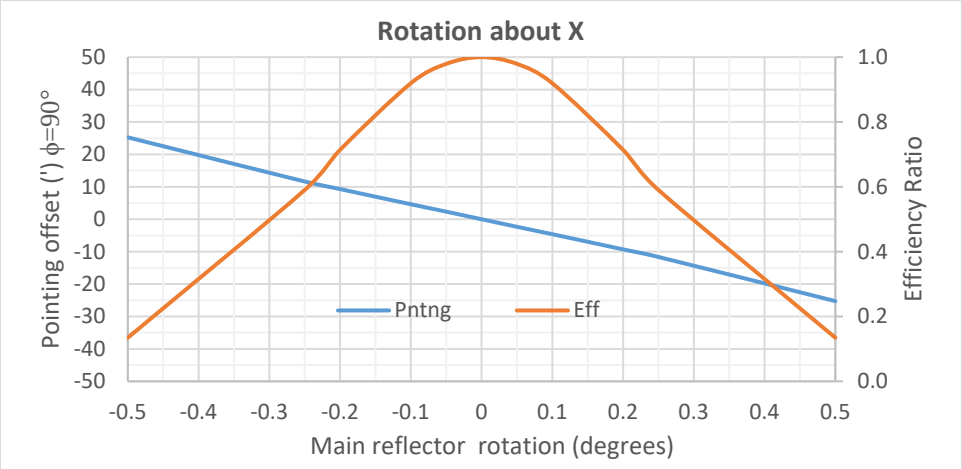

(a) Rotation about X (±0.5°)

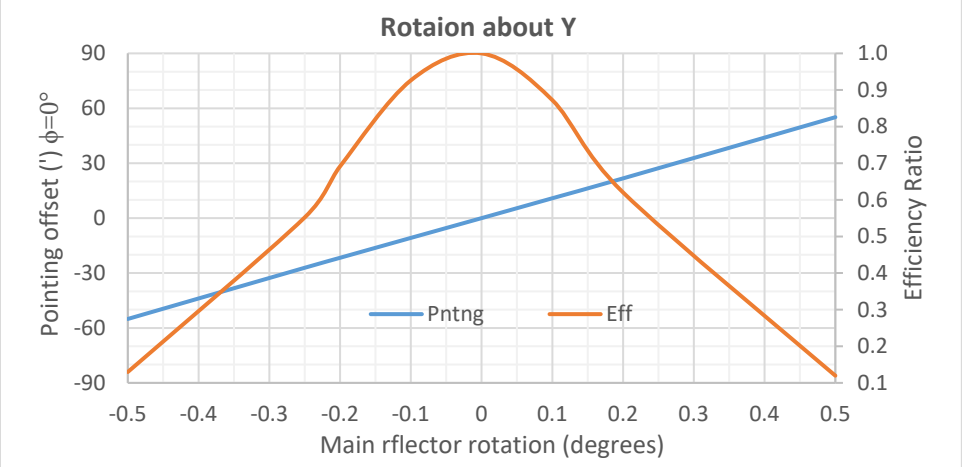

(c) Rotation about Y (±0.5°)

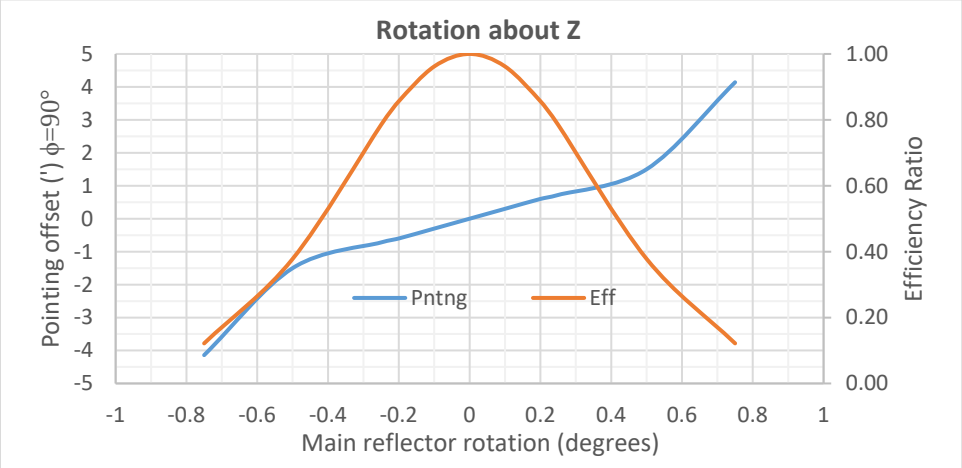

(d) Rotation about Z (±0.75°)

Figure 8. Main reflector rotations.